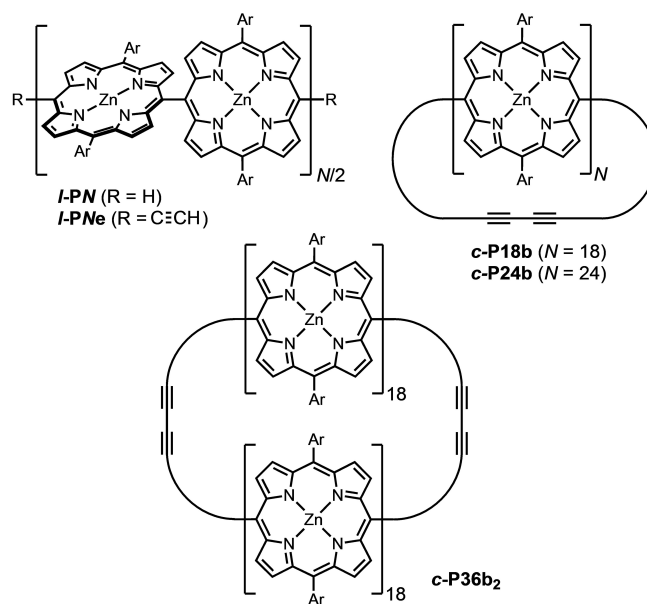


# Template-Directed Synthesis of Strained *meso-meso*-Linked Porphyrin Nanorings

Jeff M. Van Raden<sup>+</sup>, Jie-Ren Deng<sup>+</sup>, Henrik Gotfredsen<sup>+</sup>, Janko Hergenhausen<sup>+</sup>, Michael Clarke, Matthew Edmondson, Jack Hart, James N. O'Shea, Fernanda Duarte, Alex Saywell,<sup>\*</sup> and Harry L. Anderson<sup>\*</sup>

**Abstract:** Strained macrocycles display interesting properties, such as conformational rigidity, often resulting in enhanced  $\pi$ -conjugation or enhanced affinity for non-covalent guest binding, yet they can be difficult to synthesize. Here we use computational modeling to design a template to direct the formation of an 18-porphyrin nanoring with direct *meso-meso* bonds between the porphyrin units. Coupling of a linear 18-porphyrin oligomer in the presence of this template gives the target nanoring, together with an unexpected 36-porphyrin ring by-product. Scanning tunneling microscopy (STM) revealed the elliptical conformations and flexibility of these nanorings on a Au(111) surface.

Macrocycles consisting of 5,15-linked porphyrin units are fascinating targets, as precursors to edge-fused porphyrin nanobelts,<sup>[1]</sup> and because they are expected to exhibit similar ultra-fast energy migration dynamics to the chlorophyll arrays responsible for photosynthesis.<sup>[2,3]</sup> *Meso-meso*-linked linear porphyrin arrays (**I-PN**, Figure 1) behave as “photonic wires”, as a consequence of the strong exciton coupling between adjacent porphyrin units.<sup>[4]</sup> Recently, we demonstrated that a 24-porphyrin photonic wire with terminal alkyne units, **I-P24e**, can be cyclized using a non-covalent template, and that the resulting nanoring, **c-P24b**, mimics the photophysical behavior of photosynthetic light-harvesting arrays.<sup>[2]</sup> Here we demonstrate a new approach to designing templates for porphyrin nanorings by synthesizing



**Figure 1.** Chemical structures of porphyrin oligomers **I-PN**, **I-PNe**, **c-P18b**, **c-P24b** and **c-P36b<sub>2</sub>**. *N* indicates the number of porphyrin units; *l*, *c*, *e* and *b* refer to linear, cyclic, ethyne-terminated and butadiyne-linked, respectively. Ar is 3,5-bis(octyloxy)phenyl solubilizing group.

a smaller 18-porphyrin ring, **c-P18b**. This macrocycle is a challenging target because it is highly strained: the calculated strain energies of **c-P18b** and **c-P24b** are 98.0 kJ mol<sup>-1</sup> and 75.7 kJ mol<sup>-1</sup>, respectively (see Supporting Information for details of strain calculations).<sup>[5]</sup> This means that the average strain per porphyrin in **c-P18b** (5.4 kJ mol<sup>-1</sup>) is almost twice that in **c-P24b** (3.2 kJ mol<sup>-1</sup>). Furthermore, the strain is not uniformly distributed. The StrainViz tool developed by Jasti and co-workers<sup>[6]</sup> provides a visual display of the strain localization in **c-P18b** (Figure 2a; see Supporting Information for details), showing that the butadiyne bridge and the *meso* positions of the porphyrins carry the most strain. StrainViz also allowed us to integrate the strain in each porphyrin unit, revealing an alternating pattern, with the strongest alternation near the butadiyne link (Figure 2b). This pattern arises because neighboring *meso-meso*-linked porphyrin units are approximately orthogonal.<sup>[7]</sup> Alternating porphyrin units face the center of the nanoring and are more easily deformed than the porphyrin units that are approximately parallel to the

[\*] Dr. J. M. Van Raden,<sup>+</sup> Dr. J.-R. Deng,<sup>+</sup> Dr. H. Gotfredsen,<sup>+</sup> J. Hergenhausen,<sup>+</sup> Prof. F. Duarte, Prof. H. L. Anderson  
Department of Chemistry, University of Oxford  
Chemistry Research Laboratory, Oxford OX1 3TA (UK)  
E-mail: harry.anderson@chem.ox.ac.uk

M. Clarke, Dr. M. Edmondson, Dr. J. Hart, Dr. J. N. O'Shea,  
Dr. A. Saywell  
School of Physics & Astronomy, University of Nottingham  
Nottingham, NG7 2RD (UK)  
E-mail: alex.saywell@nottingham.ac.uk

[†] These authors contributed equally to this work.

© 2024 The Authors. Angewandte Chemie published by Wiley-VCH GmbH. This is an open access article under the terms of the Creative Commons Attribution License, which permits use, distribution and reproduction in any medium, provided the original work is properly cited.

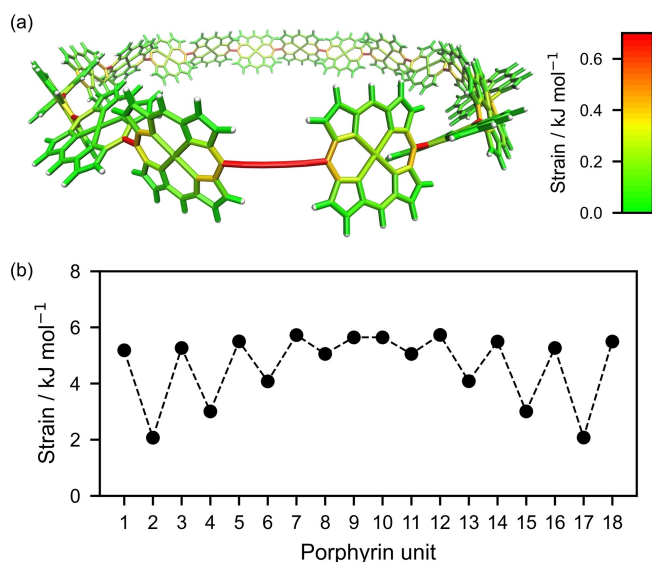


**Figure 2.** (a) StrainViz representation of the distribution of strain in **c-P18b**.<sup>[6]</sup> Strain energies were calculated using XTb as implemented in ORCA 5.0; see Supporting Information for details. The color bar was chosen to best visualize strain in the porphyrins and *meso-meso* bonds. The strain in the butadiynes (1.9–2.1 kJ mol<sup>−1</sup>) is off this scale. (b) Comparison of the total strain in each porphyrin unit. Porphyrins 1 and 18 are directly bridged by the butadiyne.

overall plane of the nanoring. Strained  $\pi$ -conjugated macrocycles often exhibit surprising behavior, because strain tends to favor conformations that maximize electronic delocalization and enhance non-covalent interactions with bound guests, as illustrated by cycloparaphenylenes.<sup>[8]</sup>

Templates have been used to synthesize many macrocycles that could not be prepared by other routes.<sup>[9,10]</sup> Alkyne-linked porphyrin nanostructures (nanorings, nanotubes and nanoballs) are particularly amenable to synthesis using radial oligo-pyridine templates.<sup>[10]</sup> However, the template-directed synthesis of nanorings consisting of *meso-meso*-linked porphyrins is more demanding, because these rod-like oligomers are difficult to bend, and neighboring porphyrin units are essentially orthogonal,<sup>[7]</sup> so that their axial coordination sites do not point towards the center of the nanoring. We began this project by designing a tridentate ligand **T3** to bind the *meso-meso*-linked trimer **I-P3** (Figure 3a). Six of these **T3** units were then connected around a central benzene core to create the 18-legged template **T18**, which has the right geometry to direct the formation of **c-P18b**. A less strained nanoring of twice the size, **c-P36b**, is formed as a by-product during the synthesis of **c-P18b**. Both **c-P18b** and **c-P36b** were characterized using a variety of techniques, including direct imaging by STM.

A range of tridentate ligands were screened computationally for their ability to bind **I-P3**, using density functional theory (DFT) at the PBE0-D3(BJ)/Def2SVP level. The most promising design, **T3** (Figure 3a), has a central *meta*-pyridine coordination site and two peripheral imidazoles connected to the benzene core via flexible  $-(CH_2)_3-$  tethers. The calculated structure of **I-P3·T3** has all three zinc centers

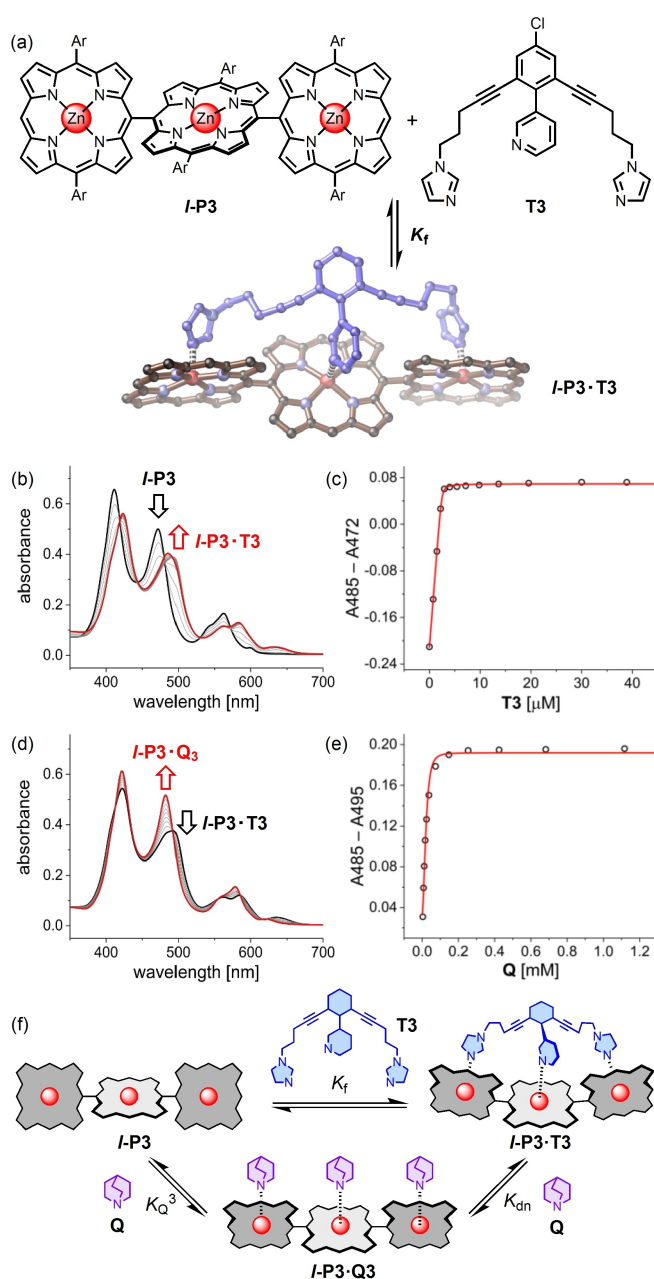


**Figure 3.** (a) Chelation of **T3** to **I-P3**; optimized geometry of **I-P3·T3** calculated by DFT (PBE0-D3(BJ)/Def2SVP); the Cl and aryl groups were replaced with hydrogen to simplify the calculation. Ar is 3,5-bis-(octyloxy)phenyl. (b) UV/Vis titration of **I-P3** with **T3** ( $[I-P3]_0 = 3.0 \mu\text{M}$ , in  $\text{CDCl}_3$  at 298 K). (c) Binding isotherm for formation of **I-P3·T3**. (d) UV/Vis titration of **I-P3·T3** with quinuclidine (**Q**). (e) Denaturation binding isotherm ( $[I-P3·T3]_0 = 3.0 \mu\text{M}$ , in  $\text{CDCl}_3$  at 298 K). In (b) and (d), the initial spectra are black and the final spectra are red. In (c) and (e), experimental points (black circles) and calculated binding isotherms (red line). (f) Thermodynamic cycle showing the formation and denaturation of **I-P3·T3**.  $K_Q$  is the binding constant for porphyrin monomer and quinuclidine ( $\log_{10} K_Q = 5.59 \pm 0.03$  in  $\text{CDCl}_3$  at 298 K).

axially coordinated, with a dihedral angle of 70–80° between neighboring porphyrin rings.

The tridentate ligand **T3** was synthesized in six steps from 4-chloroaniline (see details in Supporting

Information).<sup>[11]</sup> The interaction of **L-P3** with **T3** was tested by UV/Vis titration. Direct titration of **T3** into **L-P3** (3  $\mu$ M in CDCl<sub>3</sub> at 298 K; Figure 3b, c) indicates formation of a 1:1 complex **L-P3**·**T3** with a stability of  $\log_{10} K_f = 7.6$ . However, the association constant is too strong to determine accurately by direct titration. Denaturation titration<sup>[12]</sup> of **L-P3**·**T3** with quinuclidine **Q** as a competing ligand gave UV/Vis spectra with a set of isosbestic points, implying a two-state equilibrium from **L-P3**·**T3** to **L-P3**·**Q**<sub>3</sub> (Figure 3d). Analysis of the binding isotherms using a simple all-or-nothing model<sup>[13]</sup> gave a denaturation constant  $\log_{10} K_{dn} = 8.3$  (Figure 3e; more details in Supporting Information). The formation constant  $K_f$  for **L-P3**·**T3** was then calculated by considering the thermodynamic cycle shown in Figure 3f, giving  $\log_{10} K_f = 8.5 \pm 0.1$ . Comparison of the UV/Vis spectra of **L-P3**, **L-P3**·**T3** and **L-P3**·**Q**<sub>3</sub> shows that **L-P3**·**T3** exhibits a less intense B band (~495 nm), together with a split Q band (550–620 nm). Osuka, Kim and co-workers<sup>[14]</sup> have shown that these spectral features indicate modulation of the porphyrin-porphyrin dihedral angles, i.e. **L-P3** flattens, and the torsion angle between the porphyrin units decrease, when it binds **T3**, as predicted by our DFT calculations.

Next, we attached six **T3** units around a central benzene hub to construct the 18-legged template **T18** (Scheme 1). This synthesis started with a six-fold Suzuki coupling of the bridge unit **1** with hexakis(4-bromophenyl)benzene **2**<sup>[15]</sup> to give **3** in 74 % yield. Six-fold iridium-catalyzed C–H borylation<sup>[16]</sup> converted **3** to **4** in 81 % yield with excellent regioselectivity. Finally, **T3** was attached to the central core **4** by a second round of six-fold Suzuki coupling to generate **T18** (54 % yield).

Molecular dynamic calculations on the 1:1 complex **L-P18e**·**T18**, in explicit chloroform, indicated that coordination to all 18 zinc sites to the template would bend the linear oligomer into a circular geometry (see details in Supporting Information). The resulting complex is stable over the simulation time-scale of 300 ns and holds the terminal alkyne carbon atoms in the planar of the rest of the ring with an average distance between the alkyne terminal carbon atoms of 9.9 Å (standard deviation 3.1 Å). The closest approach of the end groups was predicted to be similar to that in the template complex used to synthesize **c-P24b**,<sup>[2]</sup> suggesting that ring closure would be feasible.

Palladium-catalyzed oxidative Glaser coupling of **L-P18e** in the presence of **T18** generated a mixture of linear and cyclic porphyrin oligomers. These oligomers were difficult to separate in the presence of the template, so the coordinated zinc was removed, together with the template, by treating the crude reaction mixture with trichloroacetic acid. The two free-base macrocyclic products, **c-P18b** and **c-P36b**<sub>2</sub>, were readily separated by recycling gel-permeation chromatography (GPC), and isolated in 7.4 % and 4.8 % yields, respectively. Zinc was quantitatively reinserted with zinc acetate prior to characterization. The larger nanoring **c-P36b**<sub>2</sub> is probably formed via a “caterpillar track” templating process, as reported for the preparation of butadiyne-linked porphyrin nanorings,<sup>[17]</sup> i.e. two equivalents of **L-P18e**·**T18** couple together to form a figure-of-eight shaped 1:2 complex **c-P36b**<sub>2</sub>·(**T18**)<sub>2</sub> (Scheme 1). Molecular dynamics

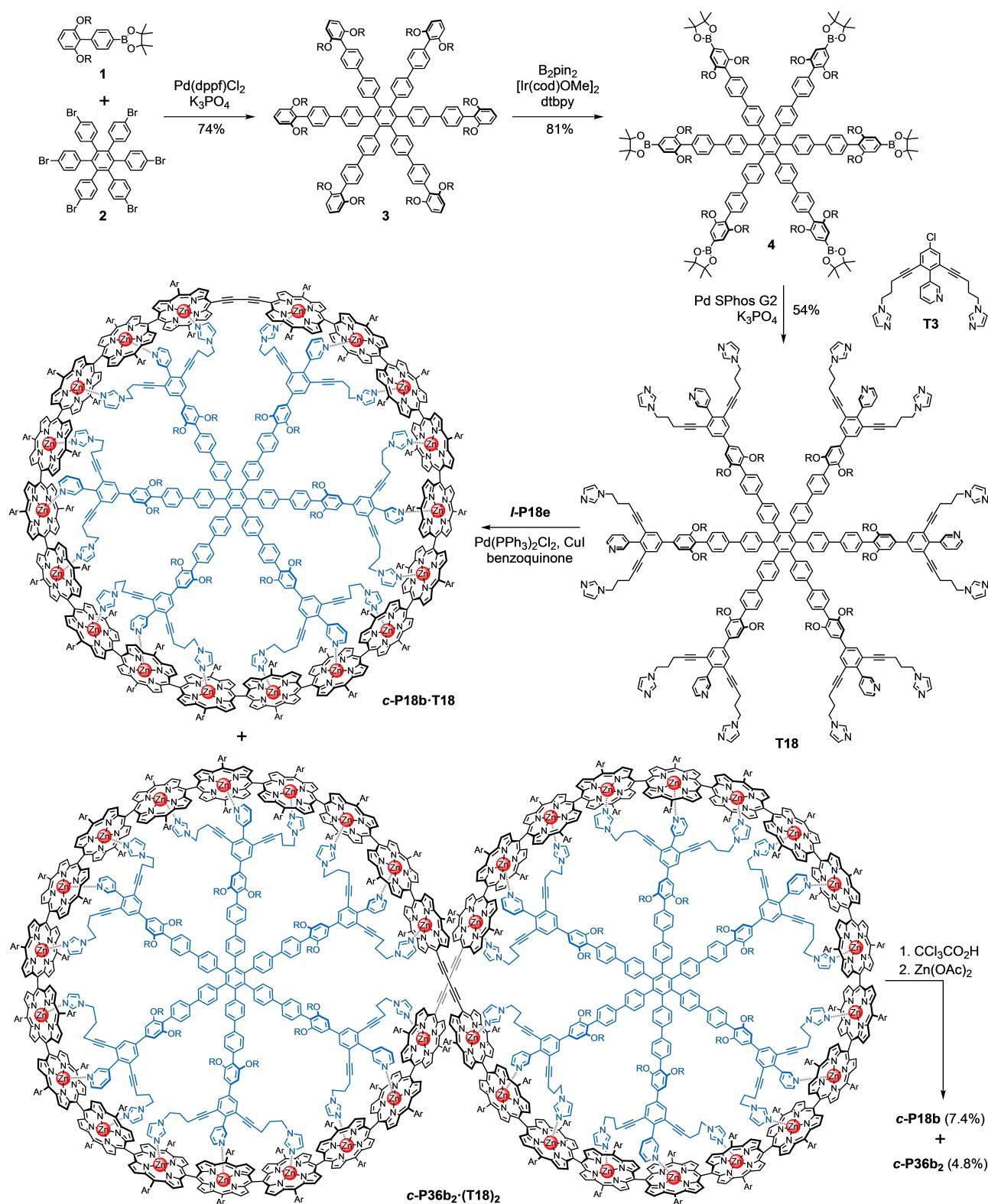
simulations show that the lemniscate configuration of **c-P36b**<sub>2</sub>·(**T18**)<sub>2</sub> is stable within the simulation time-scale, with an average angle of 51.9° between two half ring planes (Supporting Information, Figure S16).

The nanorings **c-P18b** and **c-P36b**<sub>2</sub> were first identified as cyclic oligomers from their retention times in analytical GPC. The retention times of **c-P18b** (32.6 min) and **c-P36b**<sub>2</sub> (29.4 min) are 4.5 % and 5.8 % longer than those of the corresponding linear oligomers (**L-P18e**: 31.2 min and **L-P36be**: 27.8 min), suggesting the formation of cyclic compounds with smaller hydrodynamic radii (Supporting Information Figure S5).<sup>[18]</sup> Observation of the molecular ions by MALDI ToF mass spectroscopy further supports the formation of **c-P18b** and **c-P36b**<sub>2</sub> (**c-P18b**:  $m/z$  found 18708.4, calculated C<sub>1156</sub>H<sub>1476</sub>N<sub>72</sub>O<sub>72</sub>Zn<sub>18</sub> 18709.1; **c-P36b**<sub>2</sub>:  $m/z$  found 37420.3, calculated C<sub>2312</sub>H<sub>2952</sub>N<sub>144</sub>O<sub>144</sub>Zn<sub>36</sub> 37418.3; Supporting Information Figures S40 and S41). Taken alone, the mass spectra do not prove that these molecules are cyclic, but strong evidence for cyclic structures is provided by the combination of GPC and mass spectra. The UV/Vis absorption spectra of **c-P18b** and **c-P36b**<sub>2</sub> (in toluene with 1 % pyridine) are very similar, with intense peaks at 422, 514 and 594 nm due to *meso-meso*-linked porphyrins and a small peak at 721 nm arising from the  $\pi$ -conjugated butadiyne-linked porphyrin dimer unit. The fluorescence spectra of both compounds are dominated by emission from this butadiyne-linked porphyrin dimer unit at 725 nm, demonstrating that there is efficient energy transfer to this site from all the other porphyrin units (Figure S42).<sup>[2]</sup>

Scanning tunneling microscopy (STM) provided insights into the dimensions of the **c-P18b** and **c-P36b**<sub>2</sub> nanorings, and confirmed that they are cyclic. The nanorings were transferred from solution (toluene/methanol, 3:1) onto a Au(111) surface held under vacuum during in situ electrospray deposition.<sup>[19]</sup> The STM images of **c-P18b** and **c-P36b**<sub>2</sub> (Figures 4a, b) show that the nanorings adopt ellipsoidal geometries. The measured long (*a*) and short (*b*) axis dimensions are comparable to the Zn–Zn distances for each axis from the calculated geometries (Figure 4c, d). The distributions of experimental values of *a* and *b* for **c-P18b** (41 molecules) and **c-P36b**<sub>2</sub> (59 molecules) are plotted in Figure 4e, and compared to those obtained for **c-P24b** (38 molecules).<sup>[2]</sup> The three nanorings display three distinct values for the average circumference (*c*):  $12 \pm 1$  nm for **c-P18b**,  $18 \pm 1$  nm for **c-P24b**, and  $24 \pm 3$  nm for **c-P36b**<sub>2</sub>, as expected from the different numbers of porphyrin units. The nanorings also become more flexible as the ring size increases, as indicated by the broader range of observed conformations for **c-P24b** and **c-P36b**<sub>2</sub>, compared to **c-P18b** (see scatter of data points in Figure 4e). Most of the **c-P18b** rings have a flattening factor  $f (= 1 - b/a) < 0.4$ , indicating only slight deviation from circularity, whereas **c-P24b** and **c-P36b**<sub>2</sub> display increased flattening ( $f < 0.6$  in the majority of cases) and greater flexibility.

In conclusion, we have shown that six-fold regioselective iridium-catalyzed borylation and Suzuki coupling can be used to synthesize an 18-legged template **T18** with a combination of imidazole and 3-pyridyl binding sites, that converts a twisted linear zinc porphyrin 18-mer into strained





**Scheme 1.** Synthesis of template **T18**, porphyrin nanorings **c-P18b** and **c-P36b<sub>2</sub>**. **R** = *n*-octyl; **dppf** = 1,1'-ferrocenediyl-bis(diphenylphosphine); **cod** = 1,5-cyclooctadiene; **dtbpy** = 4,4'-di-*tert*-butyl-2,2'-dipyridine; **Ar** = 3,5-bis(octyloxy)phenyl.

nanorings. The formation of nanorings **c-P18b** and **c-P36b<sub>2</sub>** was confirmed by STM. The **c-P18b** nanoring has the same number of porphyrin units as the B850 ring of light-harvest-

ing system 2 (LH2) and a similar size (5–6 nm diameter),<sup>[20]</sup> and it exhibits efficient energy transfer to the butadiyne-linked porphyrins from all the other porphyrin centers.<sup>[2]</sup>



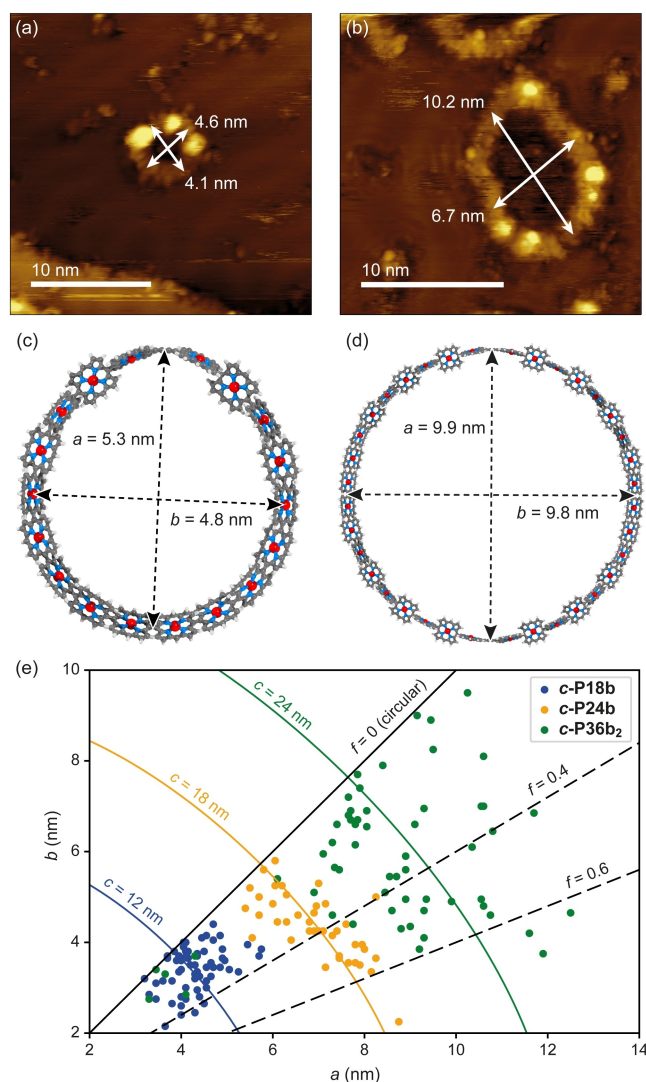


**Figure 4.** STM images of porphyrin nanorings **c-P18b** (a) and **c-P36b<sub>2</sub>** (b), deposited onto Au(111) via electrospray deposition. Imaging parameters: sample bias = −1.8 V, set-point current = 15 pA. Optimized geometry of **c-P18b** (c; PBE0-D3(BJ)/Def2SVP) and **c-P36b<sub>2</sub>** (d; PM7). Aryl and octyl groups were replaced by hydrogen to simplify the calculation. (e) Plots of experimentally measured long (*a*) versus short (*b*) axes of **c-P18b** (blue dots, 41 molecules), **c-P24b** (orange dots, 38 molecules), and **c-P36b<sub>2</sub>** (green dots, 59 molecules).  $f = 1 - b/a$  indicates the ellipticity or flattening factor of the nanorings. The blue, orange, and green arcs correspond to ellipses of fixed circumference calculated using the Ramanujan's approximations – the values are equivalent to the average circumference obtained for each nanorings. The solid black line indicates circular geometries ( $a = b, f = 0$ ). The dotted lines represent  $f = 0.4$  and  $0.6$ , the shape becoming more elliptical with increasing *f* value.

This work shows that non-covalent templates can be used to create highly strained macrocycles, and suggests strategies for the construction of templates for even larger nanorings.

## Acknowledgements

We thank the ERC (grant 885606, ARO-MAT) and EPSRC (grant EP/N017188/1) for funding, and the Oxford Advanced Research Computing (ARC) for computational resources (<https://doi.org/10.5281/zenodo.22558>). H.G. thanks the Independent Research Fund Denmark for an International Postdoctoral Fellowship (9036-00009B). A.S. thanks the Royal Society for a University Research Fellowship.

## Conflict of Interest

The authors declare no conflict of interest.

## Data Availability Statement

The data that support the findings of this study are available in the supplementary material of this article. Calculated molecular coordinates relating to this article are openly available in Zenodo at <https://doi.org/10.5281/zenodo.10451590>.

**Keywords:** porphyrinoids • nanorings • templates • scanning probe microscopy • oligomers

- [1] a) M. A. Majewski, W. Stawski, J. M. Van Raden, M. Clarke, J. Hart, J. N. O'Shea, A. Saywell, H. L. Anderson, *Angew. Chem. Int. Ed.* **2023**, 62, e202302114; b) M.-C. Yoon, Z. S. Yoon, S. Cho, D. Kim, A. Takagi, T. Matsumoto, T. Kawai, T. Hori, X. Peng, N. Aratani, A. Osuka, *J. Phys. Chem. A* **2007**, 111, 9233–9239; c) Y. Yamaguchi, *J. Chem. Phys.* **2004**, 120, 7963–7970.
- [2] H. Gotfredsen, J.-R. Deng, J. M. Van Raden, M. Righetto, J. Hergenhausen, M. Clarke, A. Bellamy-Carter, J. Hart, J. O'Shea, T. D. W. Claridge, F. Duarte, A. Saywell, L. M. Herz, H. L. Anderson, *Nat. Chem.* **2022**, 14, 1436–1442.
- [3] J. Yang, M.-C. Yoon, H. Yoo, P. Kim, D. Kim, *Chem. Soc. Rev.* **2012**, 41, 4808–4826.
- [4] a) Y. H. Kim, D. H. Jeong, D. Kim, S. C. Jeoung, H. S. Cho, S. K. Kim, N. Aratani, A. Osuka, *J. Am. Chem. Soc.* **2001**, 123, 76–86; b) J.-H. Ha, H. S. Cho, J. K. Song, D. Kim, N. Aratani, A. Osuka, *ChemPhysChem* **2004**, 5, 57–67; c) J. Yang, H. Yoo, N. Aratani, A. Osuka, D. Kim, *Angew. Chem. Int. Ed.* **2009**, 48, 4323–4327.
- [5] The total strain energy in **c-P18b** (98.0 kJ mol<sup>−1</sup>) is similar to that in cyclopropane (115 kJ mol<sup>−1</sup>) and less than that in [5]cycloparaphenylene (491 kJ mol<sup>−1</sup>) or [6]cycloparaphenylene (407 kJ mol<sup>−1</sup>) (T. Iwamoto, Y. Watanabe, Y. Sakamoto, T. Suzuki, S. Yamago, *J. Am. Chem. Soc.* **2011**, 133, 8354–8361). It is not the most strained cyclic porphyrin oligomer to be reported, and the strategy of introducing strain after macrocyclization has been used to prepare a cyclic porphyrin dimer with a strain energy of 226 kJ mol<sup>−1</sup>: Y. Xu, S. Gsänger, M. B. Minameyer, I. Imaz, D. Maspoeh, O. Shyshov, F. Schwer, X. Ribas, T. Drewello, B. Meyer, M. von Delius, *J. Am. Chem. Soc.* **2019**, 141, 18500–18507. We have also used this strategy to prepare *para*-phenylene-bridged porphyrin nanorings that are more strained than **c-P18b**: W. Stawski, J. M. Van Raden, C. W. Patrick, P. N. Horton, S. J. Coles, H. L. Anderson, *Org. Lett.* **2023**, 25, 378–383.

- [6] C. E. Colwell, T. W. Price, T. Stauch, R. Jasti, *Chem. Sci.* **2020**, *11*, 3923–3930.
- [7] a) A. Osuka, H. Shimidzu, *Angew. Chem. Int. Ed. Engl.* **1997**, *36*, 135–137; b) N. Aratani, A. Takagi, Y. Yanagawa, T. Matsumoto, T. Kawai, Z. S. Yoon, D. Kim, A. Osuka, *Chem. Eur. J.* **2005**, *11*, 3389–3404.
- [8] a) E. J. Leonhardt, R. Jasti, *Nat. Chem. Rev.* **2019**, *3*, 672–686; b) T. Kawase, H. Kurata, *Chem. Rev.* **2006**, *106*, 5250–5273.
- [9] a) J. E. Beves, B. A. Blight, C. J. Campbell, D. A. Leigh, R. T. McBurney, *Angew. Chem. Int. Ed.* **2011**, *50*, 9260–9327; b) J.-C. Chambron, J.-P. Sauvage, *New J. Chem.* **2013**, *37*, 49–57; c) J.-F. Ayme, J. E. Beves, C. J. Campbell, D. A. Leigh, *Chem. Soc. Rev.* **2013**, *42*, 1700–1712; d) J. E. M. Lewis, P. D. Beer, S. J. Loeb, S. M. Goldup, *Chem. Soc. Rev.* **2017**, *46*, 2577–2591; e) D. A. Leigh, J. J. Danon, S. D. P. Fielden, J.-F. Lemonnier, G. F. S. Whitehead, S. L. Woltering, *Nat. Chem.* **2021**, *13*, 117–122; f) T. J. Keller, C. Sterzenbach, J. Bahr, T. L. Schneiders, M. Bursch, J. Kohn, T. Eder, J. M. Lupton, S. Grimme, S. Höger, S.-S. Jester, *Chem. Sci.* **2021**, *12*, 9352–9358.
- [10] a) C. Maeda, S. Toyama, N. Okada, K. Takaishi, S. Kang, D. Kim, T. Ema, *J. Am. Chem. Soc.* **2020**, *142*, 15661–15666; b) P. S. Bols, H. L. Anderson, *Acc. Chem. Res.* **2018**, *51*, 2083–2092; c) S.-P. Wang, Y.-F. Shen, B.-Y. Zhu, J. Wu, S. Li, *Chem. Commun.* **2016**, *52*, 10205–10216; d) L. Yu, J. S. Lindsey, *J. Org. Chem.* **2001**, *66*, 7402–7419; e) S. Anderson, H. L. Anderson, J. K. M. Sanders, *Acc. Chem. Res.* **1993**, *26*, 469–475.
- [11] Y. Hirano, S. Kojima, Y. Yamamoto, *J. Org. Chem.* **2011**, *76*, 2123–2131.
- [12] C. A. Hunter, H. L. Anderson, *Angew. Chem. Int. Ed.* **2009**, *48*, 7488–7499.
- [13] H. J. Hogben, J. K. Sprafke, M. Hoffmann, M. Pawlicki, H. L. Anderson, *J. Am. Chem. Soc.* **2011**, *133*, 20962–20969.
- [14] a) N. Yoshida, D. H. Jeong, H. S. Cho, D. Kim, Y. Matsuzaki, A. Nogami, K. Tanaka, A. Osuka, *Chem. Eur. J.* **2003**, *9*, 58–75; b) H. Shinmori, T. K. Ahn, H. S. Cho, S. K. Kim, D. Kim, N. Yoshida, A. Osuka, *Angew. Chem. Int. Ed.* **2003**, *42*, 2754–2758.
- [15] R. Rathore, C. L. Burns, M. I. Deselnicu, *Org. Lett.* **2001**, *3*, 2887–2890.
- [16] a) J. F. Hartwig, *Acc. Chem. Res.* **2012**, *45*, 864–873; b) M. Nagase, K. Kato, A. Yagi, Y. Segawa, K. Itami, *Beilstein J. Org. Chem.* **2020**, *16*, 391–397.
- [17] a) M. C. O'Sullivan, J. K. Sprafke, D. V. Kondratuk, C. Rinefray, T. D. W. Claridge, A. Saywell, M. O. Blunt, J. N. O'Shea, P. H. Beton, M. Malfois, H. L. Anderson, *Nature* **2011**, *469*, 72–75; b) D. V. Kondratuk, J. K. Sprafke, M. C. O'Sullivan, L. M. Perdigo, A. Saywell, M. Malfois, J. N. O'Shea, P. H. Beton, A. L. Thompson, H. L. Anderson, *Chem. Eur. J.* **2014**, *20*, 12826–12834; c) S. Liu, D. V. Kondratuk, S. A. L. Rousseaux, G. Gil-Ramírez, M. C. O'Sullivan, J. Cremers, T. D. W. Claridge, H. L. Anderson, *Angew. Chem. Int. Ed.* **2015**, *54*, 5355–5359; d) M. Rickhaus, A. V. Jentzsch, L. Tejerina, I. Grübner, M. Jirasek, T. D. W. Claridge, H. L. Anderson, *J. Am. Chem. Soc.* **2017**, *139*, 16502–16505.
- [18] D. V. Kondratuk, L. M. A. Perdigo, A. M. S. Esmail, J. N. O'Shea, P. H. Beton, H. L. Anderson, *Nat. Chem.* **2015**, *7*, 317–322.
- [19] C. J. Judd, A. S. Nizovtsev, R. Plougmann, D. V. Kondratuk, H. L. Anderson, E. Besley, A. Saywell, *Phys. Rev. Lett.* **2020**, *125*, 206803.
- [20] R. J. Cogdell, A. Gall, J. Köhler, *Q. Rev. Biophys.* **2006**, *39*, 227–324.

Manuscript received: January 2, 2024

Accepted manuscript online: January 17, 2024

Version of record online: March 1, 2024